

High-resolution, high-reflectivity operation of lamellar multilayer amplitude gratings: identification of the single-order regime

I.V. Kozhevnikov,^{1*} R. van der Meer,² H.M.J. Bastiaens,²
K.-J. Boller² and F. Bijkerk^{2,3}

¹*Institute of Crystallography, Russian Academy of Sciences, Moscow, Russia*

²*Laser Physics and Nonlinear Optics, MESA + Institute for Nanotechnology, University of Twente, The Netherlands*

³*FOM-Institute for plasma physics Rijnhuizen, Nieuwegein, The Netherlands*

*ivk@crys.ras.ru

Abstract: High resolution while maintaining high peak reflectivities can be achieved for Lamellar Multilayer Amplitude Gratings (LMAG) in the soft-x-ray (SXR) region. Using the coupled waves approach (CWA), it is derived that for small lamellar widths only the zeroth diffraction order needs to be considered for LMAG performance calculations, referred to as the single-order regime. In this regime, LMAG performance can be calculated by assuming a conventional multilayer mirror with decreased density, which significantly simplifies the calculations. Novel analytic criteria for the design of LMAGs are derived from the CWA and it is shown, for the first time, that the resolution of an LMAG operating in the single-order regime is not limited by absorption as in conventional multilayer mirrors. It is also shown that the peak reflectivity of an LMAG can then still be as high as that of a conventional multilayer mirror (MM). The performance of LMAGs operating in the single-order regime are thus only limited by technological factors.

©2010 Optical Society of America

OCIS codes: (050.1950) Diffraction gratings; (230.4170) Multilayers; (340.0340) X-ray optics; (340.7480) X-rays, soft x-rays, extreme ultraviolet (EUV); (230.1480) Bragg reflectors

References and links

1. A. E. Yakshin, R. W. E. van de Kruis, I. Nedelcu, E. Zoethout, E. Louis, F. Bijkerk, H. Enkisch, S. Müllender, and M. J. Lercel, "Enhanced reflectance of interface engineered Mo/Si multilayers produced by thermal particle deposition", 651701:1–9, *Proc SPIE*, **6517** (2007)
2. R. A. M. Keski-Kuha, and A. M. Ritva, "Layered synthetic microstructure technology considerations for the extreme ultraviolet," *Appl. Opt.* **23**(20), 3534 (1984).
3. B. Vidal, P. Vincent, P. Dhez, and M. Nevier, "Thin films and gratings - Theories to optimize the high reflectivity of mirrors and gratings for X-ray optics", 142–149, *Proc. SPIE*, **563** (1985)
4. R. Benbalagh, J.-M. André, R. Barchewitz, P. Jonnard, G. Julié, L. Mollard, G. Rolland, C. Rémond, P. Troussel, R. Marmoret, and E. O. Filatova, "Lamellar multilayer amplitude grating as soft-X-ray Bragg monochromator," *Nucl. Instrum. Methods* **541**(3), 590–597 (2005).
5. A. Sammar, M. Ouahabi, R. Barchewitz, J.-M. André, R. Rivoira, C. Khan Malek, F. R. Ladan, and P. Guérin, "Theoretical and experimental study of soft X-ray diffraction by a lamellar multilayer amplitude grating," *J. Opt.* **24**(1), 37–41 (1993).
6. T. Peng, "Rigorous formulation of scattering and guidance by dielectric grating waveguides: general case of oblique incidence," *J. Opt. Soc. Am.* **6**(12), 1869–1883 (1989).
7. A. Coves, B. Gimeno, J. Gil, M. V. Andres, A. A. San Blas, and V. E. Boria, "Full-wave analysis of dielectric frequency-selective surfaces using a vectorial modal method," *IEEE Trans. Antenn. Propag.* **52**(8), 2091–2099 (2004).
8. L. I. Goray, "Numerical analysis of the efficiency of multilayer-coated gratings using integral method," *Nucl. Instrum. Methods* **536**(1-2), 211–221 (2005).
9. A. Sammar, J.-M. André, and B. Pardo, "Diffraction and scattering by lamellar amplitude multilayer gratings in the X-UV region," *Opt. Commun.* **86**(2), 245–254 (1991).

10. K. Krastev, J.-M. André, and R. Barchewitz, "Further applications of a recursive modal method for calculating the efficiencies of X-UV multilayer gratings," *J. Opt. Soc. Am. A* **13**(10), 2027 (1996).
 11. L. I. Goray, and J. F. Seely, "Wavelength separation of plus and minus orders of soft-x-ray-EUV multilayer-coated gratings at near-normal incidence", 81–91, *Proc. SPIE*, **5900** (2005)
 12. A. I. Erko, B. Vidal, P. Vincent, Yu. A. Agafonov, V. V. Martynov, D. V. Roschupkin, and M. Brunel, "Multilayer gratings efficiency: numerical and physical experiments," *Nucl. Instrum. Methods Phys. Res.* **333**(2-3), 599–606 (1993).
 13. V. V. Martynov, B. Vidal, P. Vincent, M. Brunel, D. V. Roschupkin, and A. Yu. Agafonov, A.I. Erko and A. Yakshin, "Comparison of modal and differential methods for multilayer gratings," *Nucl. Instrum. Methods Phys. Res.* **339**(3), 617–625 (1994).
 14. R. Benbalagh, "Monochromateurs Multicouches à bande passante étroite et à faible fond continu pour le rayonnement X-UV", PhD Thesis, University of Paris VI, Paris, 2003.
 15. I. V. Kozhevnikov, and A. V. Vinogradov, "Basic formulae of XUV multilayer optics," *Phys. Scr. T* 137–145 17, (1987).
 16. R. Petit, *Electromagnetic Theory of Gratings*, Springer-Verlag, Berlin, 1980.
-

1. Introduction

Multilayer mirrors (MM) are widely used as dispersive elements in the soft-x-ray (SXR) region. Typically, such mirrors have a spectral resolution $E/\Delta E$ in the range of 20 to 200 and a peak reflectivity of several tens of percent [1]. Absorption of SXR in the MM limits the number of bi-layers that can effectively contribute to the reflection of the incident beam and therefore limits the ultimate resolution. By fabricating a grating structure in the multilayer mirror, the penetration depth of SXR can be increased such that more bi-layers contribute to the reflection and a higher resolution can be obtained. Multilayer mirrors equipped with such a grating structure are referred to as Lamellar Multilayer Amplitude Gratings (LMAG) [2–5].

For the design of LMAGs with enhanced performance, in terms of resolution and reflectivity, adequate theory for the modeling of the diffraction of the incident SXR beam is required. At present, several rigorous approaches such as modal theory or integral method are used to simulate LMAGs [6–8], in particular in the soft X-ray region [3–5,9–14]. However, the modal theory is poorly suited for LMAGs with groove shapes that differ from rectangular or for the case of smooth interfaces between neighboring materials arising due to implantation and interdiffusion of atoms. Although the integral method described in [8] overcomes these problems, it is also stated that it is too slow to allow the modeling of gratings coated by hundreds of layers.

In this paper, we describe the results of a novel LMAG performance analysis using a coupled-waves approach (CWA) that does not have the aforementioned limitations. Its mathematical formulation is based on a general expansion of the field reflected from the LMAG, in terms of the waves diffracted into different orders, and is very understandable from the physical point of view. This CWA allows the implementation of arbitrary lamellar shapes, arbitrary depth distributions of the dielectric permittivity in the multilayer structure. In addition, it can be used without limitations on the grating period, lamellar width or number of bi-layers in the multilayer structure imposed by other models [8,10,11,13]. The CWA is well suited for calculations of LMAG performance in the soft X-ray region, because of the very small polarizability of matter in this region. This small polarizability results in very narrow reflection and diffraction peaks and negligible coupling of the reflected and diffracted waves outside the peaks. Therefore, the number of diffraction orders that need to be considered in CWA in this region is limited and computation times are quite practicable, even for multilayer structures having several thousands of layers. We would like to emphasize that in this paper, the reflectivity (zeroth order diffraction efficiency) of an LMAG is analyzed as a function of the incident angle of the incoming beam. The resolution of the LMAG is then characterized by the angular width (full width at half maximum) of the zeroth order peak.

Using the CWA presented in this paper, we derive that for small lamellar widths, LMAGs operate in a single-order regime in which there is no significant overlap of the zeroth order diffraction efficiency with higher orders. Only the zeroth order then needs to be considered when calculating the LMAG performance. We show that the reflection of a SXR wave from

an LMAG operating in this regime simply equals the reflection from a MM with a material density that is decreased with a factor equal to ratio of the lamel width to the grating period. Sophisticated diffraction theories are thus not necessary for the proper calculation of LMAG performance in the single-order regime. In contrast to what was stated in [4], we demonstrate that it is possible to derive novel analytic design criteria for LMAGs operating in the single-order regime. We also show here, for the first time, that the resolution of an LMAG operating in single-order regime is not limited by absorption, in contrast to the resolution of a conventional MM. A high resolution and high reflectivity have been shown to be mutually exclusive for a MM [15], whereas the resolution of an LMAG is only limited by technological factors and the peak reflectivity can then still be as high as for a conventional MM.

In this paper, we will first discuss the basic equations of the CWA in section 2. Next, in section 3, the results of our diffraction calculations for the LMAG in comparison to the results of other theories will be presented. Finally, in section 4, the conditions necessary for the operation of LMAGs in single-order regime will be discussed and the advantages of this regime will be presented.

2. Basic equations of the coupled waves approach

In this section, we will first derive the basic equations of the coupled-waves approach (CWA). Let us begin with defining the parameters of an LMAG and its geometrical representation as shown in Fig. 1a. Inside the lamellas, we consider a two-component (absorber A and spacer S) periodic multilayer structure (with bi-layer period d and thickness ratio γ).

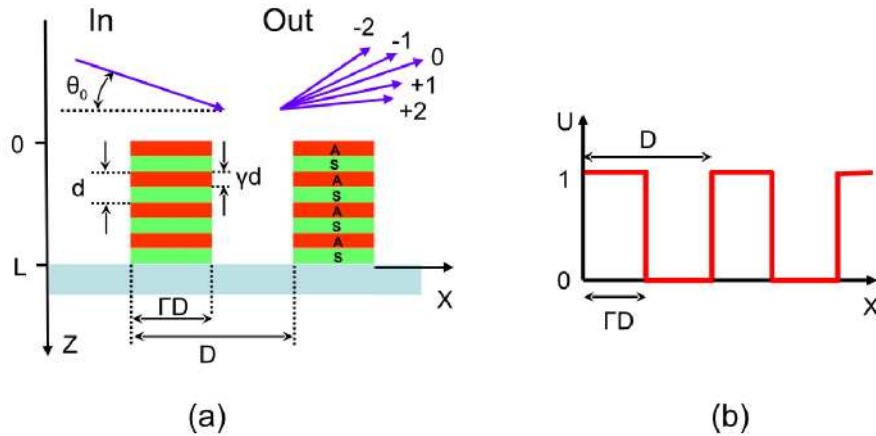


Fig. 1. Schematic of the cross section of an LMAG. (a): An incident beam from the left (In), under grazing angle θ_0 , is reflected from the multilayer and diffracted into multiple orders (Out) by the grating structure. The multilayer is built up from N bi-layers with thickness d . Each bi-layer consists of an absorber material (A) with thickness γd and a spacer material (S) with thickness $(1-\gamma)d$. The grating structure of the LMAG is defined by the grating period D and lamel width ΓD . (b): The normalized function $U(x)$ is used to describe the lamellar profile.

For simplicity, we assume that the lamellas have rectangular shapes, although the coupled waves approach described below can be extended to any lamellar shape. For brevity, we will only consider reflection and diffraction of s-polarized radiation (with the plane of incidence perpendicular to the LMAG grooves) in this paper and we will neglect the effects of interfacial roughness. The Z-axis is defined as directed into the depth of the substrate and L is the total thickness of the multilayer structure. The piece-wise periodic function U , shown in Fig. 1b, describes the lamellar profile in the X-direction normalized to L . Other functions can also be used to describe different lamellar profiles, for instance trapezoidal. The spatial distribution of the dielectric permittivity ε is then written as follows:

$$\varepsilon(x, 0 \leq z \leq L) = 1 - \chi(z) U(x; \Gamma, D); \quad \varepsilon(x, z < 0) = 1; \quad \varepsilon(x, z > L) = \varepsilon_{sub} = \text{const} \quad (1)$$

where the function $\chi(z)$ is simply the complex polarizability, which varies with depth in the multilayer structure. Although Fig. 1a, for simplicity, displays a polarizability $\chi(z)$ that varies between two values associated with materials A and S, we note that also arbitrary depth distributions of the polarizability can be used. The lamellar-profile function $U(z)$ can be expanded into the Fourier series:

$$U(x; \Gamma, D) = \sum_{n=-\infty}^{+\infty} U_n \exp(2i\pi n x / D), \quad U_0 = \Gamma, \quad U_{n \neq 0} = [1 - \exp(-2i\pi n \Gamma)] / (2i\pi n) \quad (2)$$

To analyze the diffraction pattern, we use a plane wave superposition and solve the 2D-wave equation $\nabla^2 E(x, z) + k^2 \varepsilon(x, z) E(x, z) = 0$, where the dielectric permittivity is a periodic function of x , as defined in Eqs. (1) and (2). The general solution then has the following form (chapter 1, Ref [16]):

$$E(x, z) = \sum_{n=-\infty}^{+\infty} F_n(z) \exp(iq_n x); \quad q_n = q_0 + \frac{2\pi n}{D}; \quad q_0 = k \cos \theta_0; \quad k = \frac{2\pi}{\lambda} \quad (3)$$

Here, θ_0 is the grazing angle of the incident monochromatic plane wave, q_n is the X -component of the wave vector for the n^{th} diffraction order and k is the wave number in vacuum. The boundary conditions for our problem constitute that the wave field in vacuum and in the substrate should represent a superposition of plane waves propagating at different angles to the X -axis.

Putting Eqs. (1)-(3) into the wave equation, we obtain a system of coupled differential equations and boundary conditions for the wave functions:

$$F_n''(z) + \kappa_n^2 F_n(z) = k^2 \chi(z) \sum_m U_{n-m} F_m(z) \quad (4)$$

with boundary conditions:

$$F_n'(0) + i\kappa_n F_n(0) = 2i\kappa_n \delta_{n,0}; \quad F_n'(L) - i\kappa_n^{(s)} F_n(L) = 0 \quad (5)$$

where $\kappa_n = (k^2 - q_n^2)^{1/2}$ and $\kappa_n = (k^2 \varepsilon_{\text{sub}} - q_n^2)^{1/2}$ are the Z -components of the wave vector for the n^{th} diffraction order in vacuum and in the substrate, respectively, and $\delta_{n,0}$ is the Kronecker symbol. The boundary conditions (Eqs. (5)) signify that plane waves are only incident onto the LMAG from the vacuum at a single, grazing angle θ_0 . The results discussed in the following sections were obtained by direct numerical integration of the system (4)-(5) without imposing any restriction on LMAG parameters.

Equation (4) expresses how the diffracted waves of different orders are related with each other and with the incident wave through the coefficients U_{n-m} , which characterize the lamellar profile (see Eq. (2)). For the rectangular lamel shape discussed here, the coefficients U_{n-m} are numbers. The amplitudes of the waves diffracted into the vacuum, r_n , and into the depth of the substrate, t_n , can then be found after solving Eqs. (4) and (5) to be $r_n = F_n(0) - \delta_{n,0}$ and $t_n = F_n(L)$. The interaction of the incident and diffracted waves with the multilayer structure is described in a very simple manner through the complex polarizability $\chi(z)$.

As a first test of the validity of this approach, we can insert $\Gamma = 1$ into Eq. (4), in which case the LMAG actually corresponds to a conventional multilayer mirror. All coefficients U_{n-m} then turn to zero except the coefficient U_0 , which equals 1. Equation (4) is then reduced to the simplest equation:

$$F_0''(z) + \kappa_0^2 F_0(z) = k^2 \chi(z) F_0(z) \quad (6)$$

which is indeed an ordinary 1D-wave equation describing the reflection of a wave from a MM, as would be expected.

3. Calculation of LMAG diffraction efficiency

In order to obtain an indication of the validity of our CWA, we compared our calculations of the performance of LMAGs with the results of Benbalagh et al. who used a recursive modal method [4,14]. For the comparison, we considered an LMAG based on a Mo/B₄C multilayer structure and operating at a SXR energy E of 183.4 eV. The parameters of the LMAG are: $D = 2 \mu\text{m}$, $\Gamma = 0.3$, $N = 150$, $d = 6 \text{ nm}$, and $\gamma = 0.33$. Using Eq. (4) we numerically calculated the diffraction efficiency of the zeroth order (reflectivity) $|r_0|^2$, which is shown in Fig. 2 as a function of the grazing angle of the incident wave θ_0 . The grazing incidence angle at which the highest reflectivity is obtained corresponds to the Bragg angle and for our example amounts to about 34.5° , as shown in Fig. 2f.

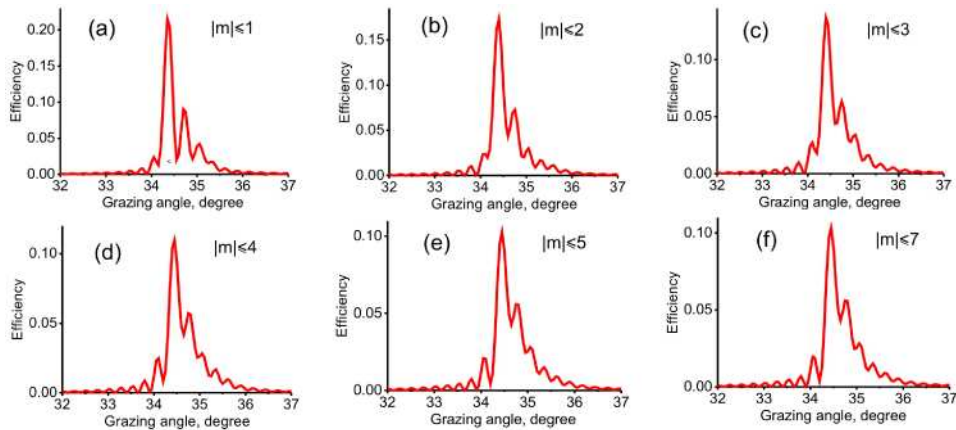


Fig. 2. Zeroth order diffraction efficiency (reflectivity) of a Mo/B₄C LMAG versus the grazing angle of an incident beam at SXR energy $E = 183.4 \text{ eV}$ for increasing number of diffraction orders taken into account when solving Eq. (4). Parameters of the LMAG: $D = 2 \mu\text{m}$, $\Gamma = 0.3$, $N = 150$, $d = 6 \text{ nm}$, $\gamma = 0.33$. The values of the complex polarizability $\chi = 1 - \varepsilon$ used for calculations: $\chi(\text{Mo}) = 2.61 \cdot 10^{-2} - i \cdot 5.77 \cdot 10^{-3}$ and $\chi(\text{B}_4\text{C}) = 4.43 \cdot 10^{-3} - i \cdot 1.08 \cdot 10^{-3}$

To obtain sufficiently accurate results within an acceptable calculation time, we must carefully choose the number of diffraction orders that will be taken into account in the calculations. In Fig. 2, we show the zeroth order reflectivity curves for an increasing numbers of diffraction orders. As can be seen in the figure, the peak value of the zeroth order diffraction efficiency first decreases and then approaches a constant value when increasing the number of diffraction orders up to 15, i.e. considering up to the $\pm 7^{\text{th}}$ diffraction order. Please note the difference in scale along the axes of the diffraction efficiency in Fig. 2. A further increase in the number of diffraction orders does neither changes the shape of the reflectivity curve nor the peak reflectivity. Such a behavior of the reflectivity curves for increasing number of diffraction orders is quite understandable from a physical point of view as incident energy must be distributed over all orders taken into account.

Figure 3 shows the diffraction efficiencies of higher orders, taking at all times up to the $\pm 7^{\text{th}}$ diffraction order into account. The figure clearly shows that the diffraction efficiency near the Bragg angle is high for the lower diffraction orders and rapidly becomes negligible for higher diffraction orders. This is a specific feature of the SXR spectral range, where the very small polarizability of materials results in very narrow reflection and diffraction peaks. We

can now conclude that for an accurate calculation of the zeroth order reflectivity curve for this specific LMAG, it is sufficient to consider up to the ± 5 th diffraction order (11 orders in total).

To test the validity of our method, we compared the calculated zeroth order reflectivity curves from our coupled-waves approach to the calculated reflectivity curves of Benbalagh et. al. [4,14]. For comparison, we included up to the $\pm 7^{\text{th}}$ diffraction order and conclude that the shape of the curves as well as the peak reflectivity are nearly identical. As an illustration, a peak reflectivity value for the zeroth order of 0.103 (see Fig. 2f) was obtained in our calculations and a value of 0.100 by Benbalagh. In our calculations the peak reflectivity decreases with increasing number of diffraction orders, whereas the results of Benbalagh show an increase. As discussed previously, a decrease in peak reflectivity is physically more understandable as energy needs to be conserved.

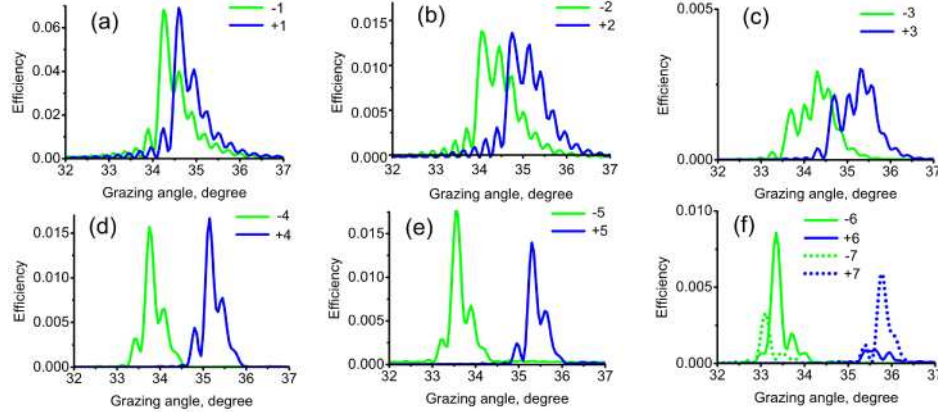


Fig. 3. Diffraction efficiencies of higher orders at $E = 183.4$ eV versus the grazing angle of the incident beam. Parameters of the LMAG are the same as for Fig. 2. At all times, 15 diffraction orders (up to $\pm 7^{\text{th}}$ order) were taken into account in the calculations.

4. LMAG single-order operating regime

The reflectivity of an LMAG can be increased by reducing the overlap of the zeroth order diffraction efficiency with higher orders. From Figs. 2 and 3, we can understand that if there is no significant overlap of these diffraction efficiencies, only negligible amounts of energy will be diffracted into higher orders and the zeroth order reflectivity will be increased. This regime will be referred to as the single-order regime.

The angular distance between diffraction peaks increases with decreasing grating period. Therefore we can expect that only the zeroth order diffraction efficiency needs to be considered for calculation of LMAG performance if the LMAG period is small enough. Equation (4) can then be reduced to:

$$F_0''(z) + \kappa_0^2 F_0(z) = k^2 \Gamma \chi(z) F_0(z) \quad (7)$$

This equation only differs from Eq. (6) by the parameter $\Gamma \neq 1$, which is inserted as a multiplier of the polarizability $\chi(z)$. As the polarizability in the SXR region is proportional to the material density, we can conclude that Eq. (7) describes the reflection of a wave from a conventional multilayer structure consisting of materials whose densities are effectively reduced by a factor of Γ .

Let us now first derive the condition for LMAG operation in single-order regime. In this regime, the angular width (full width at half maximum) of the zeroth order reflectivity peak ($\Delta\theta_{LMAG}$) should be small compared to the angular distance, in terms of the incidence angle, between the zeroth and first order diffraction peaks. This angular distance equals $\Delta\theta \approx d/D$. The angular width of the reflectivity peak of a conventional MM ($\Delta\theta_{MM}$) is determined by the

difference in the polarizabilities of the materials in the multilayer structure [15]. Hence, it decreases by a factor of Γ for a single-order LMAG, leading to $\Delta\theta_{LMAG} \approx \Gamma \cdot \Delta\theta_{MM}$. The final condition for operation in the single-order regime is then written as

$$\Gamma D \cdot \Delta\theta_{MM} \ll d \quad (8)$$

Note that condition (8) actually depends on the lamellar width ΓD rather than on the grating period D . By comparing calculated reflectivity peaks of several LMAGs with different lamellar widths, we determined that “much less” in Eq. (8) means less by a factor of 3, at least. The peak reflectivity for calculations only considering the zeroth order then differs by less than 1% compared to calculations considering many (11) orders.

To investigate LMAG operation in single-order regime, let us now consider the same Mo/B₄C LMAG as before, but with a smaller lamel width (ΓD) of 100 nm and a reduced grating period (D) of 0.3 μm (i.e. $\Gamma = 1/3$). The incident photon energy E is kept at 183.4 eV. The diffraction efficiencies of the zeroth (LMAG 0) and first (LMAG ± 1) orders are shown in Fig. 4. It is clearly visible that the angular distance ($\Delta\theta$) between the diffraction orders increases by roughly a factor of 7 as compared to Fig. 3. As a result, the diffraction efficiency of higher orders is very low near the Bragg angle where the zeroth order reflectivity is high.

Figure 4 also demonstrates that the peak reflectivity of a short-period, single-order LMAG can reach much higher values as compared to a long-period, multi-order LMAG. The peak diffraction efficiency of the short-period Mo/B₄C LMAG ($D = 0.3 \mu\text{m}$) reaches 0.38, which is almost 4 times more than the peak reflectivity of the long-period LMAG ($D = 2 \mu\text{m}$) shown in Fig. 2f. This can be explained by the re-distribution of incident intensity into the diffracted orders. In single-order operation, the incident intensity is diffracted almost entirely into one order (Fig. 4), whereas the intensity must be distributed over several orders for LMAGs with longer periods (Fig. 2). As stated previously, Eq. (8) describes the reflection of waves from a conventional multilayer structure with reduced density. This is also demonstrated in Fig. 4, where a comparison is shown between the calculated reflectivity curve for an LMAG (LMAG 0) and that for a conventional multilayer mirror (MM) with material densities reduced by a factor of $\Gamma = 1/3$. As can be seen, the agreement between the curves is excellent. In the single-order regime, sophisticated diffraction theories are thus not necessary for proper calculation of the reflectivity of an LMAG in the SXR region.

In the following, we will compare the LMAG performance, in terms of resolution and reflectivity, with the MM performance. MM performance has already been described in previous work [15]. Here, it was shown that for a MM in the SXR spectral region, the peak value of the reflectivity is completely determined by two parameters $f = \text{Re}(\chi_A - \chi_S) / \text{Im}(\chi_A - \chi_S)$ and $g = \text{Im}\chi_S / \text{Im}\chi_A$, where χ_A and χ_S are the polarizabilities of absorber and spacer. Unfortunately, Ref [15]. also showed that a high reflectivity and a high resolution are mutually exclusive for MM. The resolution of a MM can be enhanced in different manners, namely by decreasing the γ -ratio, decreasing the difference in polarizabilities of the bi-layer materials or using a MM that operates in a higher order Bragg reflection. However, all of these approaches will result in a loss of peak reflectivity and the angular resolution, which can be directly correlated to the spectral resolution, will eventually be limited by the absorption of the spacing material to:

$$(\Delta\theta_{MM})_{\min} = 2 \text{Im}\chi_S / \sin(2\theta_0) \quad (9)$$

and is only obtained for a MM with a nearly zero peak reflectivity.

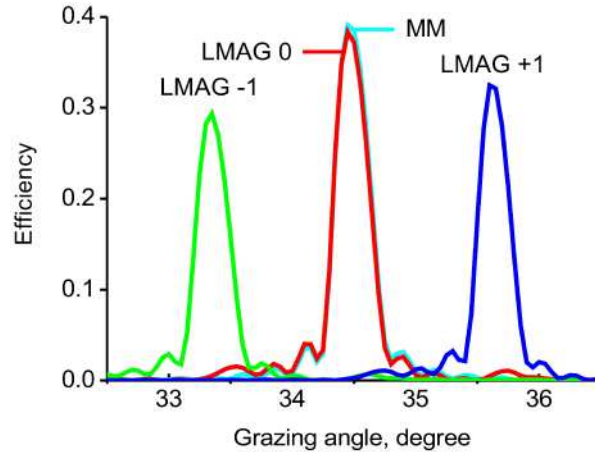


Fig. 4. Diffraction efficiency (at $E = 183.4$ eV) of the zeroth (LMAG 0) and first (LMAG ± 1) diffraction orders of a Mo/B₄C LMAG versus the grazing angle of the incident beam. The grating period $D = 0.3$ μm and the rest of the LMAG parameters are the same as for Fig. 2. In the calculations, 11 diffraction orders were taken into account. The reflectivity of a conventional Mo/B₄C multilayer mirror consisting of materials with decreased density is also shown (MM), which has an excellent agreement with the zeroth order LMAG diffraction efficiency.

However, the performance is quite different in the case of an LMAG designed to operate in the single-order regime. The angular width of an LMAG is $\Delta\theta_{LMAG} \approx \Gamma \cdot \Delta\theta_{MM}$, as was discussed when deriving Eq. (8), and the resolution is thus only limited by the Γ that can be obtained technology-wise. As stated previously, Γ can be interpreted as a reduction factor for the material density and a proportional variation in the density of both bi-layer materials does not change the parameters f and g . Hence, the peak reflectivity of an LMAG operating in the single-order regime can be the same as that of a conventional MM consisting of regular density materials. The number of bi-layers in the multilayer structure of the LMAG that is required to obtain the maximum reflectance is inversely proportional to $|\chi_A - \chi_S|$ and so must be increased by a factor of $1/\Gamma$ as compared to a conventional multilayer mirror [15].

Figure 5 illustrates these conclusions. Curve 1 shows the reflectivity curve (for $E = 183$ eV) of a conventional Mo/B₄C multilayer mirror with multilayer parameters as before (Fig. 2) and $N = 100$. The angular width of the Bragg peak is $\Delta\theta_{MM} = 0.82^\circ$. The three other curves show the reflectivity of LMAGs based on the same Mo/B₄C multilayer structure, but with different parameters Γ and D , such that the lamellar width ($\Gamma D = 70$ nm) remains the same for all LMAGs. A lamellar width of 70 nm satisfies condition (8) and is quite practicable for existing fabrication technologies. From curves 2-4, it can be seen that the width of the reflectivity curve indeed decreases by a factor of $1/\Gamma$. The angular width of curve 4 is only 0.083° , which is actually about 1.5 times less than the minimal possible angular width ($(\Delta\theta_{MM})_{\min} = 0.13^\circ$) for this MM (Eq. (9)). Yet, the peak reflectivity of the LMAGs is still the same as that of the conventional MM, although the number of bi-layers required for this is very high.

We can now state novel analytic design rules for LMAGs. If the single-order condition (8) is fulfilled, the resolution as well as the number of bi-layers required for maximum reflectance simply scale with $1/\Gamma$. There are no physical limitations on the ultimate resolution of an LMAG operating in the single-order regime and the maximum reflectance can then still be as high as for a conventional MM. Evidently, the resolution will be limited by technological factors, like the accurate deposition and etching of multilayer structures with very large numbers of bi-layers.

In this paper, we only considered the case of s-polarized radiation. However, all the main conclusions of the paper are also valid for p-polarized radiation, if $\Delta\theta_{MM}$ in Eq. (8) is the width of the Bragg peak for p-polarization.

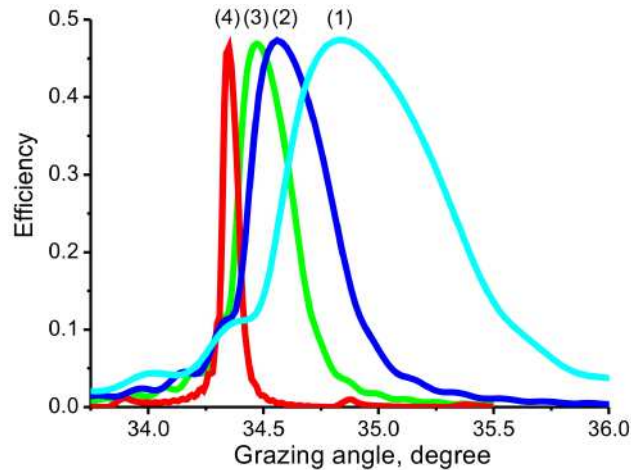


Fig. 5. Reflectivity for the zeroth diffraction order versus grazing angle (at $E = 183$ eV) for a conventional Mo/B₄C multilayer mirror (1) and three Mo/B₄C LMAGs (2-4) with the same lamellar width $\Gamma D = 70$ nm, but different Γ 's, D 's and N . (2): $\Gamma = 1/2$, $N = 200$, $D = 140$ nm; (3): $\Gamma = 1/3$, $N = 300$, $D = 210$ nm; (4): $\Gamma = 1/10$, $N = 1000$, $D = 700$ nm. The other LMAG parameters are the same as for Fig. 2. 11 diffraction orders were taken into account in the calculations.

5. Conclusions

Using our coupled waves approach (CWA), we have identified a high-resolution, high-reflectivity single-order operating regime for Lamellar Multilayer Amplitude Gratings (LMAG) for the soft-x-ray (SXR) region. In this single-order regime, the overlap of the zeroth order diffraction efficiency with higher order efficiencies is negligible. The performance, in terms of resolution and reflectivity, of LMAGs operating in the single-order regime can be calculated assuming a conventional multilayer mirror (MM) of which the material densities have been reduced by a factor of Γ (lamel-to-period ratio). For LMAGs operating in single-order, both the resolution of the LMAG as well as the number of bi-layers N required for maximum reflectance scale with $1/\Gamma$ in comparison to a conventional MM. This allowed us to define novel analytic design rules for LMAGs. We have also shown, for the first time, that the resolution and reflectivity of an LMAG are only limited by the number of bi-layers N and the lamel-to-period ratio Γ that can be obtained technology-wise. An LMAG can thus reach much higher resolutions than a conventional MM, without loss of peak reflectivity.

Acknowledgements

This research is supported by the Dutch Technology Foundation STW, which is the applied science division of NWO, and the Technology Programme of the Ministry of Economic Affairs. I.V. Kozhevnikov acknowledges the support of the ISTC (project #3124).